JOURNAL OF APPLIED ELECTROCHEMISTRY 1 (1971) 167–177

The application of electrochemical methods to the study of the electroless nickel deposition from hypophosphite solutions

C. GABRIELLI, F. RAULIN

Groupe de Recherche No. 4 du C.N.R.S., 'Physique des liquides et Electrochimie', associé à la Faculté des Sciences de Paris, 9, quai St. Bernard, Paris-5e, France

Received 30 November 1970

The rotating disk electrode has been used for the study of the electroless nickel plating from an acid bath strongly buffered by acetate. The variations of the mixed potential with the temperature have been investigated, and explained by means of polarization curves. These latter present an anodic peak which is typical of the electroless nickel deposition. The polarization resistance measurements allow a direct determination of the plating rate. All these experiments, related to mechanical measurements of plating rate, show the important inhibitor effect of the dissolved oxygen on the deposition reaction. The preliminary study of the faradaic impedance of the metal-electrolyte interface shows that the deposit occurs with not less than two heterogeneous steps, involving an adsorbed intermediate species, which could be $NiOH_{ads}$.

Introduction

As far back as 1845 the reduction of the cations Ni^{2+} by hypophosphite was observed by Wurtz [1]; however, he only obtained a black powder. The first bright plating was achieved in 1911 by Breteau [2]; then Roux [3] in 1916 took out the first patent on an electroless nickel plating bath. But these baths, using high concentrations of hypophosphite, decomposed spontaneously and led to the formation of deposit on anything which was in contact with the solution, even the walls of the container. Then several studies were carried out by Paal and Friederici [4], Scholder [5, 6], Heckel [5], and Haken [6], but their interest was in the chemical reaction itself and not in the plating mechanism. It was Brenner and Riddell [7] who discovered in 1946 the electroless nickel plating process, which is still employed. This process is based on the controlled reduction of a nickel salt solution by hypophosphite. Their first baths were basic ones: $NiCl_2.6H_2O$ 30 g/l + $NaH_2PO_2.H_2O$ 10 g/l + NH_4Cl 50 g/l + $Na_3C_6H_5O_7.5\frac{1}{2}H_2O$ 100 g/l − pH adjusted to 8–9 with NH_4OH. This led to a half-bright deposit, with a plating rate of *c.* 6 μm/h at 90°C. Thorough studies of the deposit were only carried out in the following year by Brenner and Riddell [8], both in alkaline and acid baths.

Generalities

The important developments of electroless nickel plating which have followed can be explained, not only by the fact that this plating does not need any current—which leads to industrial interest, especially for plating on non-conductive materials such as plastics—but also because of the excellent mechanical properties and uniform thicknesses of the deposits. Electroless nickel plating offers a good protection from corrosion and abrasion [8–11], which can be highly improved by a heat treatment [9, 12]. This plating is in fact a binary alloy of nickel and phosphorus

[9, 13, 14] formed by many parallel thin lamellae, each thin lamella showing a structure of perpendicular fibres to the substrate metal [9]. The structural studies by X-ray, shows that heat treatment improves the crystallization of the electroless nickel [13, 15, 16].

The characteristics of the electroless nickel plating are as follows.

(1) The nickel plating occurs only on specific surfaces. On certain metals, the reduction begins spontaneously: almost all of the group VII metals (except platinum), and metals which can displace the nickel from its solutions, such as iron [17]:

$$Fe^0+Ni^{2+}\rightarrow Fe^{2+}+Ni^0$$

On other substrates, we can initiate the deposition reaction by activating the surface with palladium chloride [18].

(2) The parameters which influence the kinetics of the deposition are numerous: temperature, pressure, pH value of solution, hypophosphite concentration, presence of different anions and certain organic substances, sample area/bath volume ratio, and stirring.

(3) The products formed by the reaction are: reduced nickel, phosphorous (2 to 20 wt%), hydrogen gas and phosphites.

(4) The structure of the deposits from acid baths, in thin lamellae of variable thickness, is more remarkable than that obtained in alkaline baths. The surface state of the substrate influences the growth of the deposit at the beginning as evidenced by Cavallotti and Salvago for alkaline baths [19].

Numerous reaction mechanisms, to interpret the stoichiometric reaction:

$$2H_2PO^-{}_2+Ni^{2+}+2H_2O\rightarrow Ni^0+2HPO^2{}_3{}^-+4H^++H_2\nearrow \quad (1)$$

have been proposed to explain the electroless nickel plating, all involving a secondary reaction of hypophosphite reduction into phosphorus, as well for acid baths as for alkaline baths.

Gutzeit [17], Brenner and Riddell [7, 8], Gorbounova and Nikiforova [20] think that hydrogen adsorbed by the catalyst is the active element for the Ni^{2+} cation reduction to metallic nickel. Ishibashi [21] assumes that the reductions of the ion H^+ to hydrogen gas and of the ion Ni^{2+} to Ni are two competing reactions, involving a reduction of the nickel without any intermediate species. Lukes [22], on the contrary, involves the presence of the ion H^-.

Cavallotti and Salvago [23], in considering the process characteristics, made an extremely interesting and critical study of a lot of the reaction mechanisms proposed in the literature to explain the electroless nickel plating. They concluded that any of the theories expressed till now cannot agree completely with the experimental facts and they proposed a more consistent mechanism represented schematically by reduction of the reactant components in two steps:

$$Ni_{aq}\cdots\left.\begin{matrix}OH\\OH\end{matrix}\right\}+H_2PO_2{}^-\rightarrow NiOH_{ads}+H_2PO_3{}^-+H \quad (2)$$

$$NiOH_{ads}+H_2PO_2{}^-\rightarrow Ni^0+H_2PO_3{}^-+H \quad (3)$$

The atomic hydrogen can perhaps transform into molecular hydrogen:

$$H+H\rightarrow H_2\nearrow \quad (4)$$

or reduce other species present in the bath, particularly hypophosphite, as Gutzeit said [17]:

$$H_2PO_2{}^-+H_{ads}\rightarrow P_{Ni}+H_2O+OH^- \quad (5)$$

One can also consider the reduction process of water by hypophosphite:

$$H_2O+H_2PO_2{}^-\rightarrow H_2PO_3{}^-+H_2\nearrow \quad (6)$$

In any case, it seems that the mechanism of the electroless nickel plating is very complicated, with several intermediate steps, including the mass transfer.

Therefore, it seemed to us very interesting to examine this kind of plating reaction by means of electrochemical methods, especially using the rotating disk electrode. This method allows the direct study of the influence of the transport by convective diffusion, and the elimination of the concentration polarization proceeding from mass transfer.

Experimental

The double jacket plating cell (Fig. 1) is made of pyrex. It contains about 250 cc of plating solu-

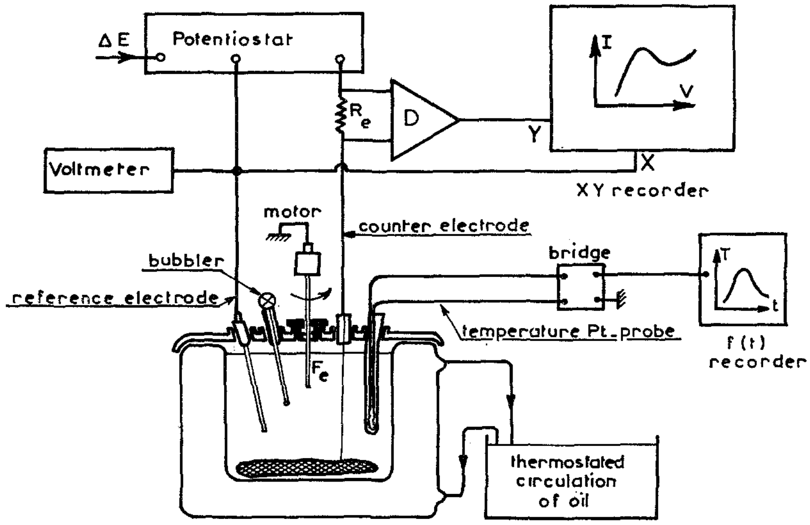

Fig. 1. Diagram of the experimental apparatus.

tion. The cell lid also in pyrex has been incorporated to make the plating cell as tight as possible. It facilitates the preparation of an air-free solution by bubbling with inert-gas, so that the concentration of dissolved oxygen is better defined. In addition, evaporation is less important, so that the ion concentrations, especially the solution pH, are well stabilized. Through this cell lid, a temperature probe, three electrodes (working, counter, and reference), and a bubbler of inert gas (argon or nitrogen), pass by conical sockets into the solution. A thermostat, set in a heat-proof tank filled up by liquid paraffin, allows the heat-carrier liquid to circulate continuously, to regulate the cell temperature. A circulation of cold water in the coil tube, also set in this tank, ensures the cooling. The increasing and decreasing rate of temperature are practically the same, and constant in the range of 30°–80°C. Besides, they are reproducible, and the fluctuations of the temperature in the steady state are better than ± 0·2°C.

As a working solution, we chose an acid bath of the Kanigen-type, corresponding to the baths which are often employed in practice, of chosen composition: $NiCl_2.6H_2O$ 20 g/l + H_2PO_2Na 20 g/l + $CH_3CO_2H/CH_3CO_2NH_4$ buffer 0·5 M + $Pb(CH_3CO_2)_2$ 1 ppm, pH = 4·5, T = 95°C (except where otherwise indicated)—filtration before plating.

For the study of the influence of temperature on the plating rate, the plating substrate is a cylindrical rod of mild steel of 5 mm diameter. The lateral surface is covered with polyolefinic thermoretractable sheath, the adherence of which with the metal is improved by a thin araldite layer. This sheath ensures the electrical insulation and prevents the deposition on the lateral surface. This cylindrical nickel sample is used as a working electrode for the electrochemical measurements. It is rotated by an asynchronous motor at constant speed. This latter is varied by means of a mechanical speed reducer; it becomes, therefore, a rotating disk electrode.

The samples to be nickel-plated are prepared by several steps described below as follows:

(1) Mechanical polishing with diamond paste (2 μm) or mechanical polishing with emery paper till 800 grade, then electrolytic polishing in 'butycellosolv' bath containing 10 wt% of $HClO_4$ during 1 h at 25 V, between −5°C and 0°C.

(2) Cold distilled water rinse.

(3) Degreasing with trichlorethylene.

(4) Cold distilled water rinse.

The temperature measurements are carried out with a Pt-probe immersed in the cell. This probe is connected to one arm of a bridge using an operational amplifier. The output of the device is connected to a digital voltmeter, which indicates directly the solution temperature, after adjusting the bridge and calibrating the Pt-probe. We can check the stability of the temperature by recording all through the nickel plating process. The potential difference, measured between a saturated calomel reference electrode and the working electrode connected to ground, is recorded on the Y shift of an XY recorder. The output of the temperature measurement device is connected to the input X. Therefore, we obtained directly and continuously the potential variation with temperature change $E = f(T)$.

For the recording of the polarization curves, we employed a platinum counter electrode of very large surface. In our laboratory we established that with such an asymmetric cell, the ohmic drop is localized in the vicinity of the working electrode. This latter is previously plated with electroless nickel during 1 h at 95°C. We use a high performance electronic potentiostat with low noise and very low drift, especially developed for faradaic impedance measurements, with the help of a correllation transfer function analyser [24]. It allows us to maintain the potential of the rotating disk electrode at a chosen value v reference electrode and check with a digital voltmeter (Fig. 1). The polarization curve is obtained potentiokinetically by superposing a voltage sweep with the potentiostat, and is recorded on an XY tracer.

The surface state studies are carried out by measuring the maximum amplitude, e_m, of the microrelief using a differential interferometer with two polarized waves. The microprofile of a nickel deposit gives an interferogram on which the central fringe is bordered on each side by black spots. The measurement of the distance $2r$ between the farthest spots allows the evaluation of the maximum depth of the microprofile [25].

The temperature influence on plating rate was studied by the measurement of the weight gain. The deposition was performed on thin rectangular and large surface mild steel sheets. This metal sheet is immersed in the plating bath vertically and hung by a nylon thread.

The influence of other variables on plating rate was studied using a rotating disk electrode. But the weight gain measurement is not sufficiently accurate enough because the weight gain is too small, owing to the limited reacting surface, compared to the total electrode mass. So we had to use another technique: once nickel plated the electrode is fixed in a mounting acrylic resin commonly used in metallurgy (Specifix—Struers) and cut off along generating lines by grinding with carborundum paper in running water with a mechanical polisher, so as not to damage the deposit structure. Then the sample, polished with the 2 μm diamond paste, is etched with dilute nitric acid during 10 s, then water-rinsed and air-dried. An observation with a metallographic microscope, using a micrometric ocular previously calibrated, allows direct measurement of the deposit thickness. For thickness values between 5 μm and 10 μm, the measurement error is about 10%; up to 10 μm, it is better than 5%.

Results and Discussion

Preliminary studies

(*a*) *Characteristics of employed bath.* The study on the variation of weight gain during one hour of Ni plating, on the large sample, in respect of temperature, shows the remarkable influence of the bath temperature on plating rate, as shown in Fig. 2. The plating time being determined is short enough for the concentrations of initial components not to be changed: the deposited mass of nickel m on the unit surface during 1h represents the plating rate dm/dt. If A, B, C, are the reacting species: $v = dm/dt = k[A]^{\alpha}[B]^{\beta}[C]^{\gamma}$ where k is the rate constant of pseudo-order 0. [A], [B], [C], being constant, save in a multiplicative factor, k is equal to v.

As illustrated in Fig. 2, k obeys Arrhenius's law: $\log k = \log k_0 - \lambda/T$.

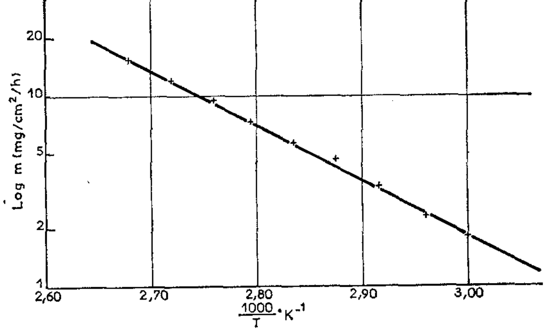

Fig. 2. Variation of the plating rate with the reciprocal of temperature. Unmoved sample; air-free solution.

The slope of the obtained curve (Fig. 2): $\lambda = 2{\cdot}8 \times 10^3\ K^{-1}$ corresponding to an activation energy: $\Delta E = 5{\cdot}6$ kcal/mole. This is in good agreement with Lee's results, relating to a fixed sample in a high buffer acetate bath [26], for which a similar calculation of ΔE gave $\Delta E = 5$ kcal/mole.

The study of the stability of plating rate with time has been made with the help of a high speed rotating disk electrode, in order to interpose the perturbation brought about by the sample rotation (particularly the evaporation of the solution). Fig. 3 represents the variation with plating time of electroless Ni weight, deposited on the electrode by the rotating speed of 3,000 rpm, in an air-free bath at 95°C. The choice of this rotation speed value will be justified later (Fig. 4). The deposition rate keeps constant up to 2 h in our plating conditions. When the plating time exceeds 3 h, we observed that the plating rate increases because the concentration of reacting species becomes more important, by the evaporation of solution water. According to these results, we chose 1 h for the experimental deposition time; this is sufficient to obtain generally an appropriate deposit thickness (greater than 10 μm), without any excessive modification of the bath composition, or of the deposition rate.

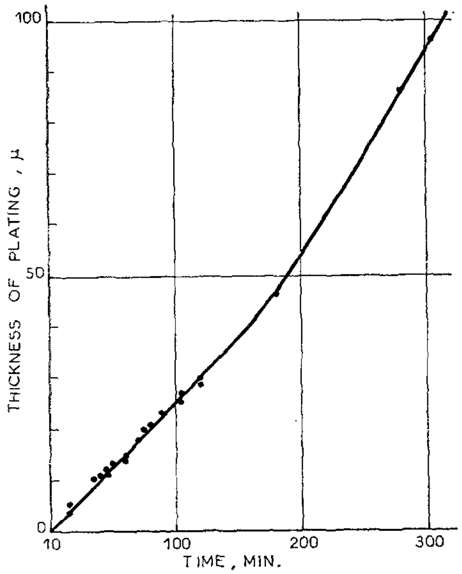

Fig. 3. Variation of the deposit thickness with the plating time. Air-free solution at 95°C; electrode rotation speed: 3,000 rpm. We have the relation $m_{mg/cm^2/h} = 0{\cdot}78\ e_u$.

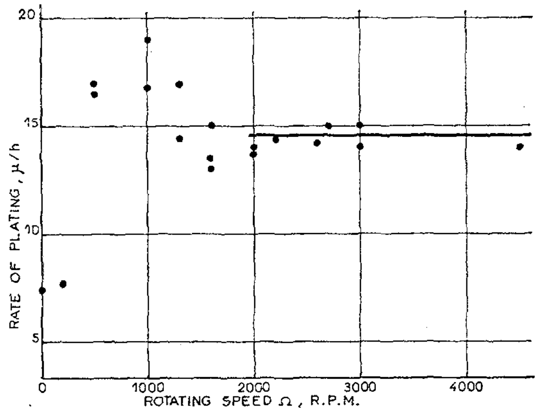

Fig. 4. Variation of the plating rate with the electrode rotation speed. Air-free solution at 95°C.

(*b*) *The influence of the rotation speed.* In order to effect a preliminary study of the influence of the rotation speed of the disk electrode on the plating rate, we have determined the thickness of the electroless nickel layer, after plating for 1 h in an air-free bath, at 95°C (Fig. 4). Up to 500 rpm the plating rate increases with rotation speed. The surface state of plating is irregular, presents important macrogeometric defects and also is of non-uniform thickness. This seems to be due to the evolution of gas at the electrode surface: the hydrogen bubbles remain in contact with the deposit and disturb the diffusion layer. A maximum appears around 1,000 rpm. This phenomenon can be related to the results obtained by Feldstein and Amodio [27], in a study of the influence of agitation on electroless plating. But instead of a rotating disk electrode, they used a rotating stirring blade, where the mass transfer process is not well-defined. But from 500 to 2,000 rpm, the results are little reproducible. When the rotating speed is faster than 2,000 rpm, the plating rate is practically constant and equal to $14{\cdot}5 \pm 0{\cdot}5$ μm/h. Therefore the electrochemical studies will be carried out, except where otherwise indicated, under a rotation speed of the disk electrode faster than 2,000 rpm.

(*c*) *The influence of substrate surface state.* Cavallotti and Salvago [19] have shown the remarkable influence of the substrate on the brightness of the deposit. Therefore, it is certain that the electrochemical studies require a perfectly definite and reproducible electrode surface state. We looked for a suitable method of the substrate preparation: thanks to an initial mechanical polishing of the substrate, using up to 2 μm diamond paste, we can obtain a reproducible microgeometric relief of the deposit. Thus the maximum amplitude e_m of the microrelief is independent of the deposit thickness, and its value is somewhere between 250 and 400 Å. Hence, the deposit is bright. However, it sometimes presents macrogeometric defects, with wrinkled spirals which wind round the rotation axis. These spirals correspond to the hydrodynamic flow at the electrode, and appear because of an irregular activity of the surface, probably due to the presence of hydrogen bubbles.

A better surface state of plating has been obtained on the electropolished substrate: most of the macrogeometric defects disappear, probably because of the high activating effect of the polishing bath used. The maximum value of the microrelief amplitude e_m is found between 200 and 250 Å which is of the same order of magnitude as the microrelief of the substrate metal and which also corresponds to the best sensitivity of the apparatus used. This value is independent of the deposit thickness. Therefore, in most of the cases, this substrate preparation method has been chosen, except when otherwise indicated.

Electrochemical study

As the electroless nickel plating does not need external current, one of the characteristic electrochemical parameters of the whole reaction is the mixed potential E_M. On the polarization curves, E_M is therefore defined by the potential value where $i = 0$. Except for the work by Gorbounova and Nikiforova [28] and Englander [29], few electrochemical studies have been made on electroless nickel deposition. Therefore, we studied the behaviour of the mixed potential, as a function of the solution temperature, by direct measurements, and also by means of polarization curves, recorded in a narrow potential range around the mixed potential.

(*1*) *Behaviour of mixed potential as a function of temperature*. Gorbounova and Nikiforova [28], have already studied the curves $E_M = f(T)$, and their dependence on the concentration of the bath products. They gradually heated the solution, and measured the potential every 5°C. They found a potential shift to more negative values. They stated that the reduction of hypophosphite will begin at this temperature as hydrogen gas evolution occurs. A direct and continuous recording of the $E_M = f(T)$ curve confirmed this result, and we discovered some sort of hysteresis phenomenon: the curves obtained by increasing or decreasing the temperature (Fig. 5) are different; and we found that this

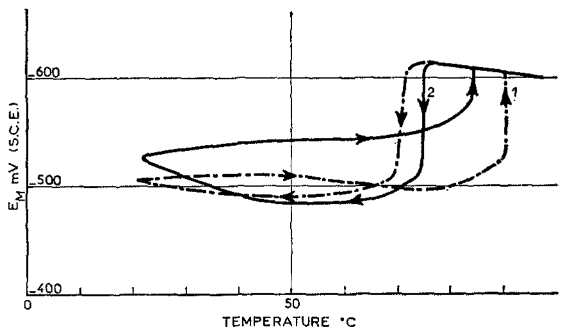

Fig. 5. Dependence of the $E_M = f(T)$ cycle and different rates of change of temperature. Under air atmosphere solution; electrode rotation speed: 2,000 rpm; rate of change of temperature (1) 3°C/mn, (2) 1°C/mn.

phenomenon depends on the rate at which temperature is varied. In fact the width of the 'hysteresis cycle' is reduced when the rate of variation of the temperature decreases (Fig. 5). Nevertheless, the transformation limit does not seem reversible, because the hysteresis phenomenon persists even when the rates of decrease and increase of temperature are extremely low. It will be noticed that the potential is more steady in the temperature range where the deposition occurs. Besides, in the case of decreasing temperature, the potential jump is very sharp. Thus we decided to restrict ourselves to the nickel plating behaviour for decreasing temperature.

The influence of dissolved oxygen on the curves $E_M = f(T)$ has been found to be very important. We bubbled inert gas, air or oxygen through the cell in order to change the oxygen concentration of the solution. The variations of the mixed potential with temperature, $E_M = f(T)$, obtained in deaerated (a), aerated (b) and oxygen saturated solution (c) are given in Fig. 6. These curves have been obtained at decreasing temperature $\Delta T/dt = -3°C$ per min, the rotating speed of disk being 2,000 rpm. In case (a), the potential jump appears around 60°C, and its amplitude is relatively small (30 mV). In case (b), the potential jump appears earlier: around 70°C, and its amplitude is more important: about 100 mV. Lastly, in case (c), the potential jump appears from 78°C, and its amplitude is larger than 200 mV. Hence, it is seen that an increase of oxygen concentration shifts the potential jump towards higher temperatures, and enlarges the jump amplitude. On the other hand, the plating rate has been determined in these three cases, by measuring the thickness of deposits obtained in 1 h at 95°C with previous solutions (a), (b), (c). It has been found to be 14 μm/h for (a), 13 μm/h for (b), but in case (c), the plating thickness is irregular and its average plating rate is 8 μm/h. Therefore, an increase of the oxygen concentration leads to a decrease of the plating rate. This seems to be due to an inhibitor effect of oxygen. This effect can be related to the results obtained by Feldstein and Amodio [34] on the oxy-anion inhibition in electroless plating. Besides comparing these results with electrochemical studies, it can be supposed that the potential jump indicates

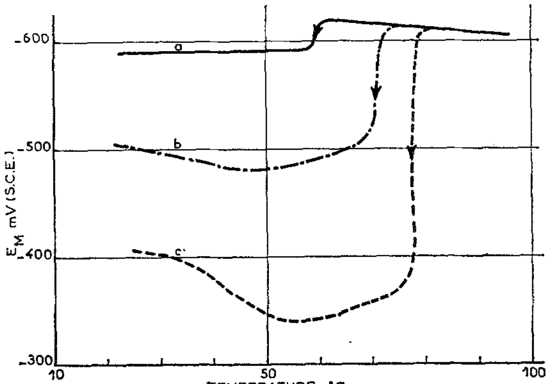

Fig. 6. Variation of the mixed potential with the temperature for different oxygen concentrations of the solution. Rate of change of temperature: -3°C/mn; electrode rotation speed: 2,000 rpm; (a) air-free solution, (b) under air atmosphere solution, (c) under oxygen atmosphere solution.

the beginning or the end of the plating reaction corresponding to increasing or decreasing temperature.

The effect of the rotation speed Ω on the $E_M = f(T)$ curves has been studied. The temperature value at the potential jump, during the decreasing variation of temperature, increases with Ω. It may be supposed that this phenomenon is also due to the effect of dissolved oxygen: the rotation speed Ω increases the rate at which oxygen diffuses towards the electrode. This parameter can be controlled by bubbling the solution with inert gas such as argon, and by using a constant rotation speed Ω.

(2) *Study of the current-potential curves.* In order to complete the results already obtained, the behaviour of the polarization curves, with respect to temperature, around the mixed potential, has been studied; that is, in a potential range corresponding to the electroless deposition reaction. The $i = f(E)$ curves present an anodic peak, which appears only at the temperatures where the electroless nickel deposition occurs (see Figs. 7 and 8). Recordings have been made

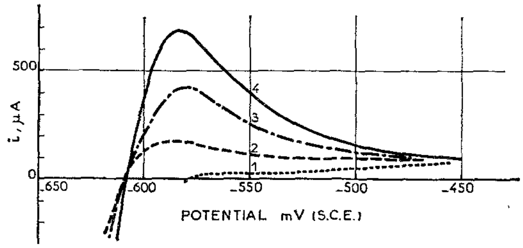

Fig. 7. Dependence of the polarization curves on the hypophosphite concentration. Air-free solution; temperature: 93°C; electrode rotation speed: 2,000 rpm; rate of potential variation: 24 mV/mn; hypophosphite concentration: (1) 2 g/l; (2) 5 g/l; (3) 10 g/l; (4) 20 g/l.

for different rotation speeds: the peak is virtually independent of diffusion rate. Besides, an increase of the Ni^{2+} concentration has little effect on the peak itself: the curves are slightly shifted to more positive potentials (and cathodic currents). On the contrary, as shown in Fig. 7, this peak depends strongly on the hypophosphite concentration. These results will be related to the concentration effect of reacting species on the plating rate; in an acid bath, the deposition rate is practically independent of the Ni^{2+} concentration, but is strongly influenced by the varia-

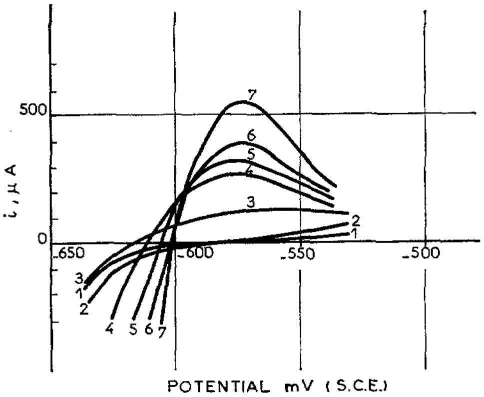

Fig. 8. Dependence of the polarization curves on temperature. Air-free solution; electrode rotation speed: 2,000 rpm; rate of change of potential: 24 mV/mn; (1) 45°C; (2) 50°C; (3) 65°C; (4) 75°C; (5) 81°C; (6) 88°C; (7) 95°C.

tions of the hypophosphite concentration [17]. It can be supposed, that this anodic peak is caused by the oxidation of adsorbed species on the electrode surface, especially the hydrogen, and that it is typical of electroless nickel plating reactions.

The variation of polarization curves with temperature, in the neighbourhood of mixed potential, is illustrated in Fig. 8. The curve $E = f(T)$ can be explained with the help of this diagram. At low temperatures, the polarization curve is very inclined to the potential axis. The mixed potential is not well-defined; it is in fact, fixed essentially by the reduction of dissolved oxygen.

When the temperature increases, the slope of the curve around the mixed potential increases while, on the other hand, the dissolved oxygen concentration decreases; thus the curve shifts slowly to more negative potentials. When the temperature range, corresponding to an appreciable deposition rate, is attained, the anodic peak, typical of the deposition, appears and fixes the mixed potential: it produces a potential jump. At higher temperatures, the anodic peak becomes more important, the slope of the polarization curve increases and the mixed potential shifts towards anodic values, as illustrated on the curves $E_{Ms} = f(T)$ (see Fig. 9). One can also explain the important influence of oxygen on these same curves. At high temperatures, as the slope of the polarization curve is important, the mixed potential is stable and less sensitive to the oxygen concentration. At low temperatures, on the other hand, as the slope of the polarization curve at E_M is small, this curve is very sensitive to the presence of oxygen: it shifts towards anodic potentials and cathodic currents by increase of the dissolved oxygen concentration in consequence of the reaction of oxygen reduction. So the mixed potential at low temperature is strongly shifted to the more anodic values. Consequently, the potential jump obtained during the temperature variations, increases with the dissolved oxygen concentration.

Regarding the current-potential curves, it can be noticed that the mixed potential value corresponding to the temperatures where the deposition occurs, is stable. And it is also noted that in this range, the potential varies very little with the temperature. Therefore, from the practical point of view, it seems there is no interest in relating the potential variations to the plating rate. On the other hand, the slope of the curves $i = f(E)$ at the mixed potential, which is equal to the inverse of the polarization resistance, varies markedly with the temperature. Moreover, in the corrosion studies, the polarization resistance is related to the corrosion rate, by means of the formula of Stern and Geary [30]. Thus, the variations of the polarization resistance R_p with temperature have been studied. We measured R_p, by superimposing a square wave of frequency 0·4 Hz with the potentiostat, on both sides of the mixed potential, and by observing the current response on an oscilloscope; the amplitude of the signals was as small as possible, in order to remain in the linear current-potential domain. The frequency chosen was low enough to attain R_p. We have verified that this value is equal to that obtained from the steady $i = f(E)$ curve. In Fig. 9, results are given relating to the polarization resistance (a and b), and to the mixed potential (a′ and b′). For decreasing temperatures, from 97° to 60°C, operating in argon atmosphere (a and a′) and in normal atmosphere (b and b′), we remark that there is a correlation between the mixed potential variations and the polarization resistance variations. For temperatures of the order of 95°C, $R_p = 20\ \Omega$ for the actual electrode surface (0·2 cm^2), and when T decreases, R_p increases and becomes very large ($R_p > 500\ \Omega$)

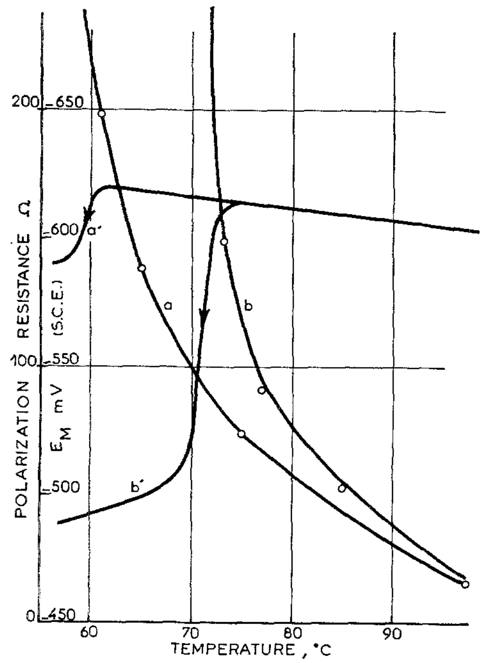

Fig. 9. Variation of the polarization resistance (a and b) and of the mixed potential (a′ and b′) with the temperature. a and a′: air-free solution; b and b′: under air atmosphere solution.

for the temperature corresponding to the potential jump. Regarding the results of the preliminary study relating to the deposition rate v, we observe that the product $R'_p(T) \cdot v(T)$ remains practically constant, where R'_p is the slope of the corrected polarization curve ($R'_p = R_p - R_e$, where R_e represents the electrolyte resistance). The curves in Fig. 9 show that, on the one hand the jump of potential corresponds to a zero rate of deposition (R_p, very large), and on the other hand that the presence of oxygen increases R_p and decreases the rate of deposition. These curves confirm the preceding results.

(3) *Study of the electrode impedance during the electroless nickel plating.* In order to obtain information about the electroless nickel plating, it is very interesting to use, in addition to the stationary electrochemical methods, a relaxation technique. The interpretation of the electrode impedance of the metal-electrolyte interface has already led to very useful information, in our laboratory [31, 32], particularly in the case of electrolytic nickel plating [31]. The mechanisms proposed in the literature involving electrochemical reactions can be studied by this method. As the previous investigation allowed us to work under very reproducible conditions, we have carried out a preliminary study of the deposition mechanism by the faradaic impedance analysis.

The experimental device is shown in Fig. 1; it uses, in addition, a correlation transfer function analyser [24]. We can obtain directly the real part R and the imaginary part G of the electrode impedance Z at each measuring frequency, the generator giving ΔE and the correlator analysing Y (Fig. 1). $Z = R - jG$ is plotted in the complex plane. The plating is carried out under an argon atmosphere, at 98°C; the electrode rotation speed is equal to 2,300 rpm.

The faradaic impedance diagram is given in Fig. 10. We remark that, when the measuring

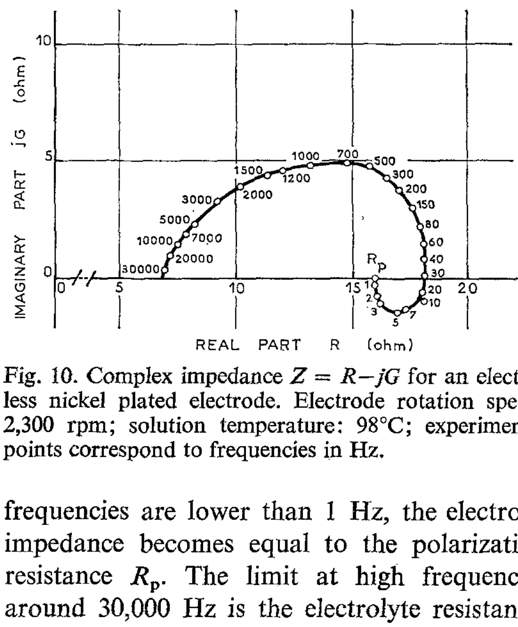

Fig. 10. Complex impedance $Z = R - jG$ for an electroless nickel plated electrode. Electrode rotation speed: 2,300 rpm; solution temperature: 98°C; experimental points correspond to frequencies in Hz.

frequencies are lower than 1 Hz, the electrode impedance becomes equal to the polarization resistance R_p. The limit at high frequencies around 30,000 Hz is the electrolyte resistance, which is equal to 7 Ω. It is observed that the impedance diagram is composed of two parts: the high frequency part, which corresponds to the double-layer capacity, and the low frequency part, which corresponds to an inductive term. This latter is generally due to the relaxation of the electrode coverage by an adsorbed intermediate species [31–33]. This result can be connected to the mechanism set up by Cavallotti and Salvago [23], which involves the adsorbed intermediate species $NiOH_{ads}$. This intermediate adsorbed species may play an important role, as is the case in the mechanism for the electrocrystallization of nickel in acid solution (Watts bath) [31].

Conclusion

In seeking to ascertain the different parameters which influence electroless nickel plating, we were able to obtain reproducible conditions for nickel plating, particularly in relation to the surface state of the deposit, and the overall reaction rate. Thus we were able to make reproducible measurements of electrode potentials and polarization curves, as well as impedance diagrams.

The potential jump observed on the curve $E_M = f(T)$ is related to the plating rate: at decreasing temperature, it corresponds to the arrest of the plating reaction; the reduction of oxygen occurs instead of the nickel reduction. For increasing temperatures, we suppose that the potential jump shows the beginning of the plating reaction.

The polarization curves have an anodic peak, which increases with the plating rate, and disappears when the plating reaction ceases. This peak is typical of the electroless nickel plating.

The polarization resistance measurements allow a direct determination of the plating rate.

Finally, we made clear the inhibiting effect of the dissolved oxygen on the deposition reaction. We think that this can be attributed to the oxidation of the electroless nickel on the sample surface. From the practical point of view, it is possible to increase the electroless nickel deposition rate, by working with an air-free bath.

The preliminary study of the faradaic impedance diagram shows that the deposit occurs with not less than two heterogeneous steps, involving an adsorbed intermediate species, which may be $NiOH_{ads}$. A thorough study of the impedance of the metal–electrolyte interface, particularly as a function of temperature around the mixed potential, should give more definite information about the electroless nickel plating process.

Acknowledgment

The authors wish to thank P. Dr. I. Epelboin, Director of their laboratory for stimulating discussions and helpful comments.

References

[1] A. Wurtz, *C.R. Acad. Sci. Paris*, **18** (1844) 702; **21** (1845) 149.
[2] P. Breteau, *Bull. Soc. Chim.*, **9** (4) (1911) 515.
[3] F. G. Roux, *U.S. Patent* (1916) 1207–218.
[4] C. Pall and L. Friederici, *Ber. Deut. Chem. Ges.*, **64** (B) (1931) 1766.
[5] R. Scholder and H. Heckel, *Z. Anorg. Allgem. Chem.*, **198** (1931) 329.
[6] R. Scholder and H. L. Haken, *Ber. Deut. Chem. Ges.*, **64** (B) (1931) 2870.
[7] A. Brenner and G. E. Riddell, *J. Res., N.B.S.*, **39** (1946) 1.
[8] A. Brenner and G. E. Riddell, *ibid.*, **39** (1947) 385.
[9] A. Brenner, C. Cohen, G. Gutzeit, A. Krieg, W. H. Metzger, W. H. Safranek, E. B. Saubestre, C. F. Waite, and W. E. Moline, 'Symposium on Electroless Nickel Plating', Special Technical Publication no. 265, A.S.T.M. (1959).
[10] B. I. Pantukh and B. G. Ossovskij, *Zh. Prikl. Khim., SSSR*, **41** (2) (1968) 432.
[11] T. Shimizu and S. Ishibashi, *Metal Finishg. Soc. Jap.*, **19** (10) (1968) 418.
[12] A. V. Rjabchenkov, V. V. Ovsjankin, and Ju. A. Zot' Ev, *Zashchi. Metallov. SSSR*, **5** (6), (1969) 638.
[13] A. W. Goldenstein, W. Rostoker, F. Schossberger, and G. Gutzeit, *J. Electrochem. Soc.*, **104** (2) (1957) 104.
[14] J. P. Randin, E. Saurer, P. A. Moire, and H. E. Hintermann, *ibid.*, **114** (5) (1967) 442.
[15] K. T. Zielke, W. S. Dritt, and C. H. Mahoney, *Metal. Progress*, **77** (1960) 84.
[16] A. H. Graham, R. W. Lindsay, and H. J. Read, *J. Electrochem. Soc.*, **112** (1965) 401.
[17] G. Gutzeit, *Plating*, **46** (1959) 1158; 1275; 1377; **47** (1960) 63.
[18] A. Brenner, *Metal Finishg.*, **52** (11) (1954) 68; (12) (1954) 61.
[19] P. Cavallotti and G. Salvago, *Electrochimica Metallorum*, **111** (1968) 23.
[20] K. M. Gorbounova and A. A. Nikiforova, *Zhur. Fiz. Khim.*, **28** (1954) 883.
[21] S. Ishibashi, *Himeji Kogyo Daigaku Kenkyu Hokoku*, **13** (1961) 68; C.A. **56** (1961) 1283.
[22] R. M. Lukes, *Plating*, **51** (1964) 969.
[23] P. Cavallotti and G. Salvago, *Electrochimica Metallorum*, **111** (1968) 239; (1968) 338.
[24] I. Epelboin, C. Gabrielli, and J. C. Lestrade, *Rev. Gen. Elec.*, **79** (1970) 669.
[25] M. Froment and R. Wiart, *Electrochim. Acta*, **8** (1963) 481.
[26] W. G. Lee, 'Factors affecting the Phosphorus Content of Chemical Nickel Deposits'. Congress on Metallic Corrosion, (1966) 711.
[27] N. Feldstein and P. R. Amodio, *Plating*, **56** (1969) 1246.
[28] K. M. Gorbounova and A. A. Nikiforova, *Zashch. Metallov*, **1** (1965) 63.

[29] I. Englander, Ph.D University of Connecticut Engineering, Chemical (1966).
[30] M. Stern and A. L. Geary, *J. Electrochem. Soc.*, **104** (1) (1957) 56.
[31] R. Wiart, Thèse de Doctorat d'Etat, Paris (1968) No. d'enregistrement C.N.R.S.: AO 2605.
[32] M. Keddam, Thèse de Doctorat d'Etat, Paris (1968) No. d'enregistrement C.N.R.S.: AO 2192; *idem, Traitements de Surface*, **95** (1969) 39; **96** (1970) 3.
[33] I. Epelboin and M. Keddam, *J. Electrochem. Soc.*, **117** (8) (1970) 1052.
[34] N. Feldstein and P. R. Amodio, *ibid*, **117** (9) (1970) 1110.